

SPECTROSCOPIC STUDY OF $^{161,163}\text{Er}$ IN DEFORMED HARTREE–FOCK THEORY

B.B. SAHU, S.K. SINGH, S.K. PATRA, C.R. PRAHARAJ

Institute of Physics, Sachivalaya Marg, Bhubaneswar-751 005, India

M. BHUYAN, Z. NAIK

School of Physics, Sambalpur University, Jyotivihar, Sambalpur-768 019, India

S.K. GHORUI

Department of Physics and Meteorology, IIT Kharagpur
Kharagpur-721 302, India

(Received October 17, 2011; revised version received January 9, 2012)

The rotational bands of $^{161,163}\text{Er}$ are studied by deformed Hartree–Fock and angular momentum projection techniques. Energy spectra and the matrix elements of electromagnetic operators are calculated up to high spin values $J = 59/2$ and compared with experimental measurement wherever available. The $B(E2)$ and $B(M1)$ values for some of the bands are evaluated.

DOI:10.5506/APhysPolB.43.451

PACS numbers: 21.10.Dr, 21.10.Ft, 21.10.Gv, 21.10.Tg

1. Introduction

Nuclear rotational motion is a remarkable example of correlated single particles in a deformed field generating a collective mode. For odd-mass rotational nuclei the coupling of single-particle and collective rotational degrees of freedom leads to a rich variety of band structures [1,2]. The study of high spin states in deformed odd- N nuclei is interesting because of the coupling of odd neutron to the deformed core and the role of large j orbits giving rise to many bands extending to high spins. For finer description of the states in deformed nuclei, such as band-crossing, rotation-alignment and signature effects in the spectra and electromagnetic transitions *etc.*, one needs a many-body description of the system using two-body interaction among nucleons.

Nuclei in the mass region $A \sim 135$ are transitional in nature with moderate deformation and soft with respect to the triaxially parameter (γ). There are large number of positive-parity orbitals originating from the $g_{7/2}$, $d_{5/2}$, $d_{3/2}$, and $s_{1/2}$ spherical shell-model states which can be seen in Nilsson diagrams. This determines the low-energy structure, whereas for the negative-parity states there is only the $h_{11/2}$ orbital. Many of these nuclei show interesting spectroscopic properties both at low and high spins [3, 4, 5, 6].

In the odd-mass even- Z nuclei ($N = 77$), collective structures based on the $h_{11/2}$ and $g_{7/2}$ neutron configurations have been systematically observed and characterized as having a triaxial prolate shape [7, 8]. Recently, $^{152-158}\text{Nd}$ [4, 9] and ^{137}Ce [10] nuclei have been studied up to high spin states. Both these nuclei have shown bands based on multiquasiparticle configuration and shape coexistence phenomenon. In earlier works, some low-spin states in Sm, Gd and Dy were observed in Coulomb excitation [11]. Very recently, interesting experimental studies were done for ^{161}Er nucleus, where the high-spin states have been investigated [12]. This work motivates us to analyse the detail high-spin structure of this nucleus.

Here, we have studied the multiquasiparticle bands at high spins of $^{161,163}\text{Er}$ using Deformed Hartree–Fock (DHF) and Angular Momentum Projection technique to study the spectra, electromagnetic matrix elements and K -isomers. Spins and parities of the levels have been assigned from Hartree–Fock orbit. The calculated results have been compared with available experimental data.

This paper is organized as follows: A brief theoretical formalism and numerical calculations are presented in Sec. 2. The results and discussions are given in Sec. 3. In this section the details of the energy spectra are given and compared with the available experimental data. The electromagnetic properties of various bands are also discussed. Finally we conclude our work in Sec. 4.

2. Theoretical framework

2.1. Deformed Hartree–Fock (DHF)

A deformed single-particle state is a superposition of states of various j . Assuming axial symmetric deformation the deformed single-particle wave function can be expressed as [13]

$$|\alpha m\rangle = \sum_j C_j^{\alpha m} |jm\rangle. \quad (1)$$

The mixing amplitudes C s are the variational parameters in Hartree–Fock theory leading to energy minimization. Because of axial symmetry, K (projection of j on symmetry axis) is a good quantum number. In the uncoupled

representation, the Hartree–Fock equations are [14, 15, 16, 17]

$$(\epsilon_j - e_{\alpha m})C_j^{\alpha m} + \sum_{j_2 j_3 j_4 m_2} V(j_3 m_3 j_2 m_2; j m j_4 m_4) \rho_{j_4 m_2 j_2 m_2} C_{j_1}^{\alpha m_3} = 0. \quad (2)$$

Here ϵ_j is the single particle energy, $e_{\alpha m}$ is the Lagrange multiplier, and V is the two-body interaction among nucleons. The density matrix is defined as

$$\rho_{j_4 m_2 j_2 m_2} = \sum_{\alpha(\text{occupied})} C_{j_2}^{\alpha m_2} C_{j_4}^{\alpha m_2}. \quad (3)$$

Substituting $m_3 = m$ and $m_4 = m_2$ for axially symmetry case, equations (1) and (2) are solved self-consistently. The Slater determinants for protons and neutrons are the deformed intrinsic state $|\phi_K\rangle$.

2.2. Angular Momentum Projection

A deformed shape such as the one described by $|\Phi_K\rangle$ is localized in angle and, by the uncertainty principle, is not a state of good angular momentum (J). Thus $|\Phi_K\rangle$ does not have a unique J quantum number and is a superposition of various J states [14, 17, 18]

$$|\Phi_K\rangle = \sum_I C_{IK} |\Psi_{IK}\rangle. \quad (4)$$

One needs to project out states of good angular momenta from the intrinsic state Φ_K with the Angular Momentum Projection operator

$$P_K^{IM} = \frac{2I + 1}{8\pi^2} \int d\Omega D_{MK}^I(\Omega) R(\Omega). \quad (5)$$

Here $R(\Omega)$ is the rotation operator $e^{-i\alpha J_z} e^{-i\beta J_y} e^{-i\gamma J_z}$ and Ω represents the Euler’s angles α , β and γ . The Euler’s angles α and γ are integrated out because of axial symmetry, but the remaining one θ has to be integrated numerically. It is important to restore rotational symmetry by such projection operator. As pointed out by Peierls and Yoccoz in their original paper [18], the wave function obtained by using such projection operator gives the correct number of degrees of freedom of a many particle system, since the extra three Euler angles are integrated out to give a state of good angular momentum. The Hamiltonian and multiple matrix elements are given as follows

$$\begin{aligned} \langle \Psi_{K_2}^I | H | \Psi_{K_1}^I \rangle &= \frac{2I + 1}{2} \frac{1}{\left(N_{K_1 K_1}^I N_{K_2 K_2}^I \right)^{1/2}} \\ &\times \int d\theta \sin \theta d_{K_2 K_1}^I(\theta) \langle \phi_{K_2} | H e^{-i\theta J_y} | \phi_{K_1} \rangle, \quad (6) \end{aligned}$$

$$N_{K_1 K_2}^I = \frac{2I+1}{2} \int d\theta \sin \theta d_{K_2 K_1}^I(\theta) \langle \phi_{K_2} | e^{-i\theta J_y} | \phi_{K_1} \rangle, \quad (7)$$

$$\begin{aligned} \langle \Psi_{K_1}^{I_1} || T^\lambda || \Psi_{K_2}^{I_2} \rangle &= \frac{(2I_2+1)(2I_1+1)^{1/2}}{2 \left(N_{K_1 K_1}^{I_1} N_{K_2 K_2}^{I_2} \right)^{1/2}} \sum_{\nu} C_{K_1-\nu \nu K_1}^{I_2 \lambda I_1} \\ &\times \int_0^\pi d\theta \sin \theta d_{K_1-\nu K_2}^{I_2}(\theta) \langle \Phi_{K_1} | T_\nu^\lambda e^{-i\theta J_y} | \Phi_{K_2} \rangle, \quad (8) \end{aligned}$$

where the $N_{KK'}^I$ stands for wave function overlap (for details refer to [14, 15, 16, 17, 19, 20, 21]). The matrix element of the nuclear Hamiltonian contains single-particle and two-body residual interaction terms between two states of angular momentum J projected from intrinsic states ϕ_{K_2} and ϕ_{K_1} . The tensor operator T^L denotes of an electromagnetic operators $E2$, $M1$, etc. The integrations are done in a Gauss–Legendre quadrature with 64 points and the kernels of various quantities are solved from equations (6)–(8).

2.3. Band mixing

In general, two states $|\Psi_{K_1}^{JM}\rangle$ and $|\Psi_{K_2}^{JM}\rangle$ projected from two intrinsic configurations are not orthogonal to each other even if $|\Phi_{K_1}\rangle$ and $|\Phi_{K_2}\rangle$ are orthogonal. Thus, whenever necessary, we orthonormalize them and then diagonalize to do band-mixing using the following equation

$$\sum_{K'} (H_{KK'}^J - E_J N_{KK'}^J) C_{K'}^J = 0. \quad (9)$$

Here $C_{K'}^J$ is the orthonormalized amplitude which can be identified as the band mixing amplitude.

2.4. The deformed single particle configuration

The experimental observations call for theoretical study of the spectra and electromagnetic transitions from a microscopic point of view, so that the various features of these bands are understood on the basis of their microscopic structures. In order to obtain reliable wave function of the various bands, we should have the corresponding multiparticle states built on deformed single particles. One should also have states of good angular momentum for the various states that can be identified with the states obtained in experiment. To obtain the deformed single-particle states we have to include the residual two-body interaction among nucleons in the theoretical

The resulting HF orbits of protons and neutrons corresponding to the lowest prolate solution of $^{160,162}\text{Er}$ are shown in Fig. 1. From this figure, the single particle orbits of the next odd nucleus near the Fermi surface are identified and different band mixing between various orbitals are performed. The calculated results are presented in Figs. 2–5.

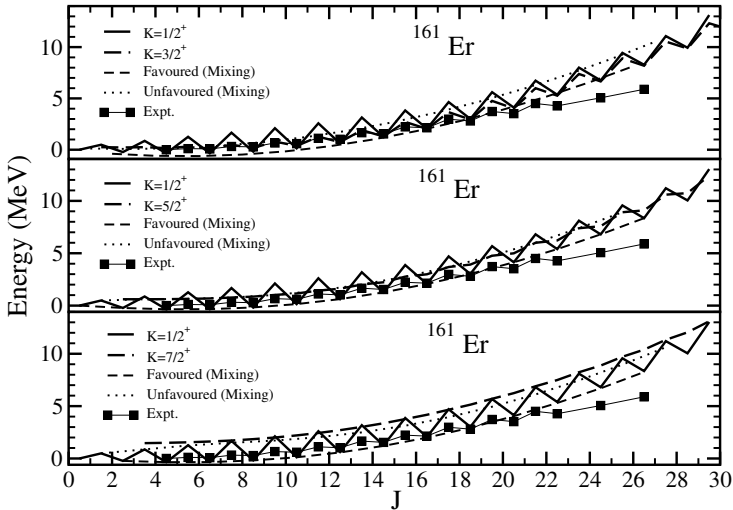


Fig. 2. Band mixing of $K = \frac{1}{2}^+$ with $\frac{3}{2}^+$ in the upper panel, $K = \frac{1}{2}^+$ with $\frac{5}{2}^+$ in the middle one and $K = \frac{1}{2}^+$ with $\frac{7}{2}^+$ in the lower panel of ^{161}Er . The experimental values are also shown for comparison [12].

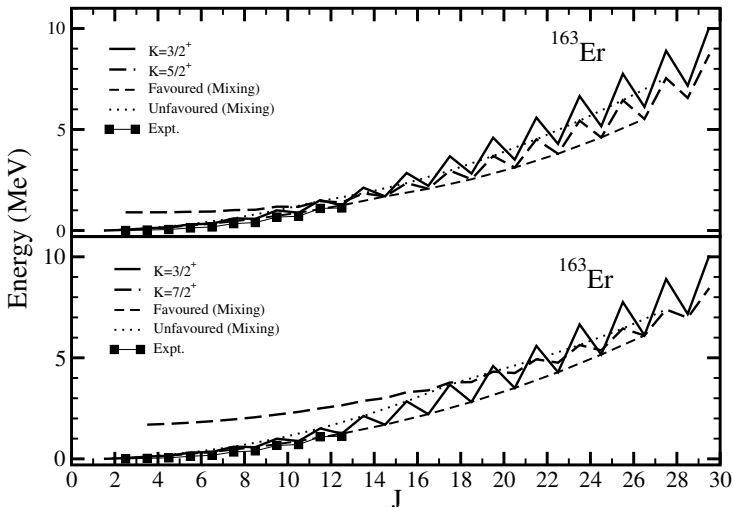
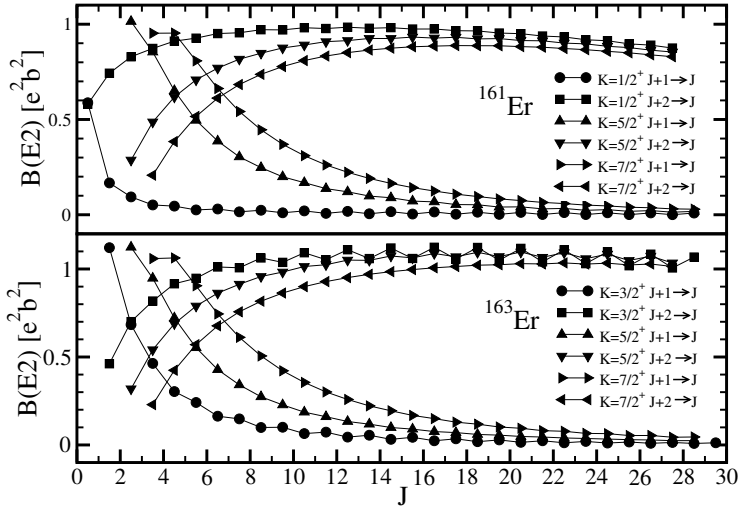
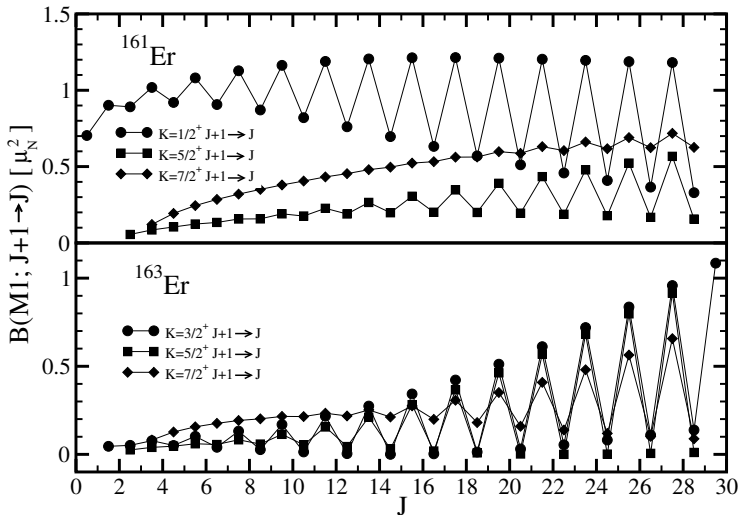


Fig. 3. Band mixing of $K = \frac{3}{2}^+$ with $\frac{5}{2}^+$ in the upper panel, and $K = \frac{3}{2}^+$ with $\frac{7}{2}^+$ in the lower panel of ^{163}Er . The experimental values are also shown for comparison [26].

Fig. 4. $B(E2)$ values of various bands of $^{161,163}\text{Er}$.Fig. 5. $B(M1)$ values of various bands of $^{161,163}\text{Er}$.

3. Results and discussion

Before going to the high spin state, we calculate the ground state binding energy (BE), root mean square charge radius (r_{ch}), and quadrupole deformation parameter β_2 for $^{161,163}\text{Er}$. We employed the most successful relativistic mean field (with NL3 parameter set) [22] and non-relativistic Skyrme Hartree–Fock (with SkI4 force) [23] formalisms to get an idea of the ground state structures of these two neutron-deficit nuclei. The calculated results are displayed in Table I. The experimental data are also given in the table for

comparison, wherever available. The RMF(NL3) results are calculated with and without taking pairing into account. A simple BCS pairing scheme is adopted. The line with an asterisk (*) is without taking pairing into account. From the table, it is clear that a couple of MeV added to the total binding energy both to the prolate and oblate solution when we included the pairing effects. On the other hand, the radius and the quadrupole deformation changes marginally.

TABLE I

Ground state binding energy (BE), root mean square charge radius r_{ch} and quadrupole deformation parameter β_2 of $^{161,163}\text{Er}$ with relativistic mean field (NL3 set) [22] and non-relativistic Skyrme Hartree-Fock (SkI4 force parameter) [23] formalisms. The experimental binding energy is taken from Ref. [24]. Energy is in MeV and r_{ch} is in fm. The line with an asterisk (*) is the result obtained without taking BCS-pairing. All other data in the table are done with BCS pairing approach.

Nucleus	BE [MeV]	r_{ch} (fm)	β_2	BE _{expt.}
NL3				
$^{161}\text{Er}^*$	1312.0	5.204	0.289	1311.482
^{161}Er	1314.0	5.214	0.293 (0.243-HF) (0.27-[25])	
$^{161}\text{Er}^*$	1305.6	5.187	-0.217	
^{161}Er	1308.7	5.198	-0.226	
SkI4				
$^{161}\text{Er}^*$	1307.7	5.168	0.278	
^{161}Er	1309.4	5.184	0.306	
$^{161}\text{Er}^*$	1302.8	5.208	-0.304	
^{161}Er	1304.4	5.205	-0.295	
NL3				
$^{163}\text{Er}^*$	1327.4	5.219	0.292	1327.591
^{163}Er	1329.7	5.239	0.316 (0.255-HF) (0.28-[25])	
$^{163}\text{Er}^*$	1321.0	5.206	-0.229	
^{163}Er	1323.7	5.218	-0.238	
SkI4				
$^{163}\text{Er}^*$	1323.9	5.205	0.310	
^{163}Er	1325.3	5.216	0.325	
$^{163}\text{Er}^*$	1318.0	5.232	-0.300	
^{163}Er	1320.0	5.199	-0.244	

After knowing the ground state properties of the nuclei $^{161,163}\text{Er}$, we proceed for the high spin effects of these nuclei. It is evident that the deformed nuclei have collective rotational bands with energies varying as $J(J+1)$ and these bands are known as regular rotational bands. Although perfect rotors and rotational spectra are rare, many of these bands show approximate rotational behaviour with the energies changing in a regular fashion with angular momentum. In general, low K bands show deviations from this regular rotational behaviour, particularly if the deformed orbits near the Fermi surface are of large j origin. In this case a band is split into two different signatures with energy staggering between the two signature branches. Here, we have used the above deformed Hartree–Fock and Angular Momentum Projection formalism to calculate the band structures (energies, $B(E2)$, and $B(M1)$ values of rotational bands) for the isotopes of Er. The energy spectra associated with each intrinsic state is obtained by angular momentum projection in the given model space and with surface delta residual interaction, using the formalism discussed in Sec. 2.

From the Hartree–Fock single-particle energy levels, it is clear that the active orbits near the Fermi surface are $3/2^+$, $5/2^+$, $7/2^+$ *etc.* There is maximum possibility of mixing of these bands with the ground one $1/2^+$. Thus we perform band mixing of these states and the results of the energy spectra are shown in Figs. 2 and 3. The $K = 1/2^+$, $3/2^+$, $5/2^+$, and $7/2^+$ bands and their mixing for both favoured and unfavoured bands along with the experimental data for the ground band is given. Our band mixing results match pretty well with the data. It is to be noted that, contradict to expectation, the band mixing result of $K = 1/2^+$ and $3/2^+$ band does not produce reasonable experimental data. That is the favoured band is a little away from the data at lower J while the unfavoured one shows a large discrepancy at higher J value. This gives enough indication to consider only the mixing of $K = 1/2^+$ with $5/2^+$ and $7/2^+$ respectively. The lower panel of the figure is for the band mixing $J^\pi = 1/2^+$ and $7/2^+$ with the experimental data are also shown for comparison. In this case also the calculated results agree well with the experimental values. Similarly, the calculated bands for $K = 3/2^+$, $5/2^+$ and $K = 3/2^+$, $7/2^+$ for ^{163}Er are presented in the upper and lower panel of Fig. 3. The band mixing of $J^\pi = 3/2^+$ with $5/2^+$ and $J^\pi = 3/2^+$ with $7/2^+$ are shown including the experimental data wherever available. The experimental data agree well with the favoured band of the band mixing results.

Apart from the energy spectra we have calculated the reduced transition matrix elements $B(E2)$ and $B(M1)$ using Eqs. (11) and (12) for these two nuclei $^{161,163}\text{Er}$. The quantity $B(E2)$ for a transition from an initial state αJ_1 to final state βJ_2 is given by

$$B(E2; \alpha J_1 \rightarrow \beta J_2) = \frac{1}{2J_1 + 1} \left| \sum_{i=p,n} \langle \Psi_{K_2}^{\beta J_2} || Q_2^i || \Psi_{K_1}^{\alpha J_1} \rangle \right|^2. \quad (11)$$

Here the summation is for quadrupole moment operators of protons and neutrons. The effective charges of $1.7e$ and $0.7e$ are used for protons and neutrons, respectively, for our calculations. The calculated results are depicted in Fig. 4. The favoured $B(E2)$ value decreases with J and at about $J \sim 14$ attains a constant quantity. On the other hand, this $B(E2)$ transition matrix element increases up-to certain value and attains the saturation at the same $J \sim 14$ for both $^{161,163}\text{Er}$.

The reduced magnetic dipole transition moment between initial and final state is given by

$$B(M1; \alpha J_1 \rightarrow \beta J_2) = \frac{1}{2J_1 + 1} \frac{3}{4\pi} \left| \sum_{i=p,n} \langle \Psi_{K_2}^{\beta J_2} || g_\ell^i \ell_i + g_s^i s_i || \Psi_{K_1}^{\alpha J_1} \rangle \right|^2, \quad (12)$$

where g_ℓ and g_s are orbital and spin g -factor respectively. The g -factor of $g_\ell = 1.0\mu_N$ and $g_s = 5.586 \times 0.5\mu_N$ for protons and $g_\ell = 0\mu_N$ and $g_s = -3.826 \times 0.5\mu_N$ for neutrons are used for $B(M1)$ calculations. The $B(M1)$ values are gradually increasing with J for both the $^{161,163}\text{Er}$ are shown in Fig. 5. The results show an increasing in zig-zag path with J for both the considered nuclei. This zig-zag nature is due to the large signature effect of these $K = 1/2^+$ (^{161}Er) and $K = 3/2^+$ (^{163}Er). The signature decreases with higher K and it is minimum for $K = 7/2^+$.

4. Summary and conclusion

In summary, we studied the high spin states of the neutron-deficit $^{161,163}\text{Er}$ odd mass nuclei. These nuclei have interesting quadrupole deformation properties and band structures. We have presented results of these nuclei using the microscopic model of Hartree–Fock and angular momentum projection technique. Our results correlate well with known experimental findings about the spectra of these nuclei. Using our Projected HF model with band mixing, we predict many bands up-to high spin values. The spectra of both $^{161,163}\text{Er}$ as well as electromagnetic properties like $B(E2)$ and $B(M1)$ are obtained.

We have shown the behaviour of $B(E2)$ for ground state and K -isomer bands for the nuclei studied in this paper. The $B(E2)$ value of the ground state band of both the considered Er isotopes were found to be smoothly varied with increasing J . The $B(E2; J + 1 \rightarrow J)$ for g.s. band had the same trend for both the isotopes studied here. For other bands in the case

of $J + 2 \rightarrow J$ transition the values were increasing with J and after a certain spin it was nearly constant. These results can be useful in future experimental studies of these nuclei. As a whole, our microscopic model can be very useful to study the band structure and electromagnetic properties in this mass region.

This work is supported in part by the UGC-DAE-CSR, Kolkata Center, India (Project No. UGC-DAE CRS/KC/CRS/2009/NP06/1354) and Project No. SR/S2/HEP-37/2008, DST, the Government of India.

REFERENCES

- [1] A. Bohr, B.R. Mottelson, *Nuclear Structure*, W.A. Benjamin, Inc., Vol. II.
- [2] R.M. Lieder, H. Ryde, *Advances in Nuclear Physics*, edited by M. Baranger, E. Vigt, Plenum, New York 1978, Vol. 10.
- [3] C.M. Petrache *et al.*, *Nucl. Phys.* **A617**, 228 (1997).
- [4] S. Kumar *et al.*, *Phys. Rev.* **C76**, 014306 (2007).
- [5] S.J. Zhu *et al.*, *Phys. Rev.* **C62**, 044310 (2000).
- [6] C. Rossi Alvarez *et al.*, *Phys. Rev.* **C54**, 57 (1996).
- [7] T.L. Khoo *et al.*, *Phys. Rev. Lett.* **76**, 1583 (1996); R.V.F. Janssens *et al.*, *Nucl. Phys.* **A645**, 191 (1999).
- [8] R.A. Bark *et al.*, *Nucl. Phys.* **A644**, 29 (1999).
- [9] S. Ogaza *et al.*, *Nucl. Phys.* **A559**, 100 (1993).
- [10] P. Kemnitz *et al.*, *Nucl. Phys.* **A209**, 271 (1973).
- [11] C. Foin *et al.*, *Nucl. Phys.* **A199**, 129 (1973).
- [12] L. Chen *et al.*, *Phys. Rev.* **C83**, 034318 (2011).
- [13] B.R. Mottelson, S.G. Nilsson, *Mat. Fys. Skr. Dan: Vid. Selsk.* **1**, (1959) and references therein.
- [14] Z. Naik, C.R. Praharaaj, *Phys. Rev.* **C67**, 054318 (2003).
- [15] C.R. Praharaaj *Structure of Atomic Nuclei*, edited by L. Satpathy, Narosa, New Delhi 1999 p. 108; C.R. Praharaaj, *Phys. Lett.* **B119**, 17 (1992); C.R. Praharaaj, *J. Phys.* **G14**, 843 (1988).
- [16] Z. Naik, Ph.D. Thesis, Institute of Physics, Bhubaneswar, 2006.
- [17] G. Ripka, *Advances in Nuclear Physics*, edited by M. Baranger, E. Vogt, Plenum, New York 1968, Vol. I, page 183.
- [18] R.E. Peierls, Y. Yoccoz, *Proc. Phys. Soc.* **A70**, 381 (1957).
- [19] C.R. Praharaaj, S.B. Khadkikar, *Phys. Rev. Lett.* **50**, 1254 (1983); C.R. Praharaaj, S.B. Khadkikar, *J. Phys.* **G6**, 241 (1980).
- [20] A.K. Rath, C.R. Praharaaj, S.B. Khadkikar, *Phys. Rev.* **C47**, 1990 (1993); A.K. Rath, C.R. Praharaaj, *Pramana* **36**, L125 (1991).

- [21] A.K. Rath, P.M. Walker, C.R. Praharaaj, *World Scientific Series on Advances in Quantum Many Body Theory* **6**, 246 (2002); C.R. Praharaaj, *Band Structure of Nuclei in Hartree-Fock Theory*, Institute for Nuclear Theory Workshop on Nuclear Many-body Theories in the 21st Century, University of Washington, Seattle, 2007.
- [22] G.A. Lalazissis, J. König, P. Ring, *Phys. Rev.* **C55**, 540 (1997).
- [23] J. Rikovska Stone *et al.*, *Phys. Rev.* **C68**, 034324 (2003).
- [24] G. Audi, Wang Meng, private communication, April 2011.
- [25] P.H. Stelson, L. Grodzins, *Nucl. Data* **A1**, 21 (1965).
- [26] S.A. Hjorth *et al.*, *Nucl. Phys.* **A144**, 513 (1970).